Membraneless Unbuffered Seawater Electrolysis for Pure Hydrogen Production

Nan-Nan Liang and Hyunwoong Park*
School of Energy Engineering, Kyungpook National University, Daegu 41566, Republic of Korea
*To whom correspondence should be addressed:
Tel: +82-53-950-8973; E-mail: hwp@knu.ac.kr

Table S1. Comparison of electrochemical ClOR in saline water

Catalyst	Electrolyte	Onset potential	ClOR FE (%)	Stability test	Ref
Pt_1/CNT	1 M NaCl + 0.1 M $HClO_4$	1.38 V vs. RHE	94% J = 10 mA cm^{-2}	12 h J = 10 mA cm^{-2}	1
RuO_2/CC-10	5 M NaCl	1.05 V vs. SCE			2
$Ti_{0:35}V_{0:35}Sn_{0:25}Sb_{0.05}O_x$	5 M NaCl + 0.01 M HCl	1.25 V vs. Ag/AgCl		20 h J = 400 mA cm^{-2}	3
$RuTiO_x$	4.0 M NaCl at pH 2	1.32 V vs. NHE	94.8% J = 100 mA cm^{-2}	250 h J = 100 mA cm^{-2}	4
$CoSb_2O_x$	4.0 M NaCl at pH 2	1.60 V vs. NHE	97.4% J = 100 mA cm^{-2}	250 h (100 mA cm^{-2})	4
$RuIrTiO_x$	4 M NaCl	1.12 V vs. Ag/AgCl	90% J = 400 mA cm^{-2}		5
$RuTiSnSbO_x$	5 M NaCl	1.18 V vs. SCE			6
BDD/RuO_2	2 M NaCl	1.08 V vs. SCE			7
RuO_2–Sb_2O_5–SnO_2	Seawater	1.20 V vs. SCE	90.4% J = 250 mA cm^{-2}	266 h J = 1 A cm^{-2}	8
RuO_2-IrO_2-SnO_2-Sb_2O_5	Seawater	1.15 V vs. SCE	84.2% J = 1 A cm^{-2}	658 h J = 2 A cm^{-2}	9
Sb-SnO_2/IrTaOx/TiO_2 TNT	1 M NaCl	1.80 V vs. NHE	95% J = 10 mA cm^{-2}	100 h J = 10 mA cm^{-2}	10
PRT ($Pt_{0.06}Ru_{0.24}Ti_{0.7}O_y$)	0.137 M NaCl	0.99 V vs. SCE	100% J = 80 mA cm^{-2}		This study
	0.5 M NaCl	0.99 V vs. SCE	100% J = 80 mA cm^{-2}		

	Seawater	0.99 V vs. SCE	100% J = 80 mA cm^{-2}		
	0.941 M NaCl	0.95 V vs. SCE	100% J = 80 mA cm^{-2}	500 h J = 800 mA cm^{-2}	

References

1. T. Lim, G. Y. Jung, J. H. Kim, S. O. Park, J. Park, Y. Kim, S. J. Kang, H. Y. Jeong, S. K. Kwak & S. H. Joo, Atomically dispersed Pt–N_4 sites as efficient and selective electrocatalysts for the chlorine evolution reaction, *Nat. Commun.* 2020, 11, 412

2. F. Zhang, X. Gu, S. Zheng, H. Yuan, J. Li, X. Wang, Highly catalytic flexible RuO_2 on carbon fiber cloth network for boosting chlorine evolution reaction, *Electrochim. Acta,* 2019, 307, 385-392

3. M. M. Alavijeh, S. Habibzadeh, K. Roohi, F. Keivanimehr, L. Naji, M. R. Ganjali, A selective and efficient precious metal-free electrocatalyst for chlorine evolution reaction: An experimental and computational study, *Chem. Eng. J.* 2021, 421, 127785

4. I. A. Moreno-Hernandez, B. S. Brunschwig and N. S. Lewis, Crystalline nickel, cobalt, and manganese antimonates as electrocatalysts for the chlorine evolution reaction, *Energy Environ. Sci.* 2019, 12, 1241

5. A. R. Zeradjanin, N. Menzel, W. Schuhmann and P. Strasser, On the faradaic selectivity and the role of surface inhomogeneity during the chlorine evolution reaction on ternary Ti–Ru–Ir mixed metal oxide electrocatalysts, *Phys. Chem. Chem. Phys.* 2014, 16, 13741

6. K. Xiong, Z. Deng, L. Li, S. Chen, M. Xia, L. Zhang, W. Ding, S. Tan, X. Qi, Z. Wei, Sn and Sb co-doped RuTi oxides supported on TiO_2 nanotubes anode for selectivity toward electrocatalytic chlorine evolution, *J. Appl. Electrochem.* 2013, 43, 847-854

7. S. Ferro and A. D. Battisti, Electrocatalysis and Chlorine Evolution Reaction at Ruthenium Dioxide Deposited on Conductive Diamond, *J. Phys. Chem. B*, 2002, 106, 2249-2254

8. S. Chen, Y. Zheng, S. Wang, X. Chen, Ti/RuO_2–Sb_2O_5–SnO_2 electrodes for chlorine evolution from seawater, *Chem. Eng. J.* 2011, 172, 47-51

9. S. Wang, H. Xu, P. Yao, and X. Chen, Ti/RuO_2-IrO_2-SnO_2-Sb_2O_5 Anodes for Cl_2 Evolution from Seawater, *Electrochemistry (Tokyo)*, 2012, 80(7), 507-511

10. Y. Lee, Y. Park, Ultrathin multilayer Sb-SnO_2/$IrTaO_x$/TiO_2 nanotube arrays as anodes for the selective oxidation of chloride ions, *J. Alloys Compd.* 2020, 80, 155622.

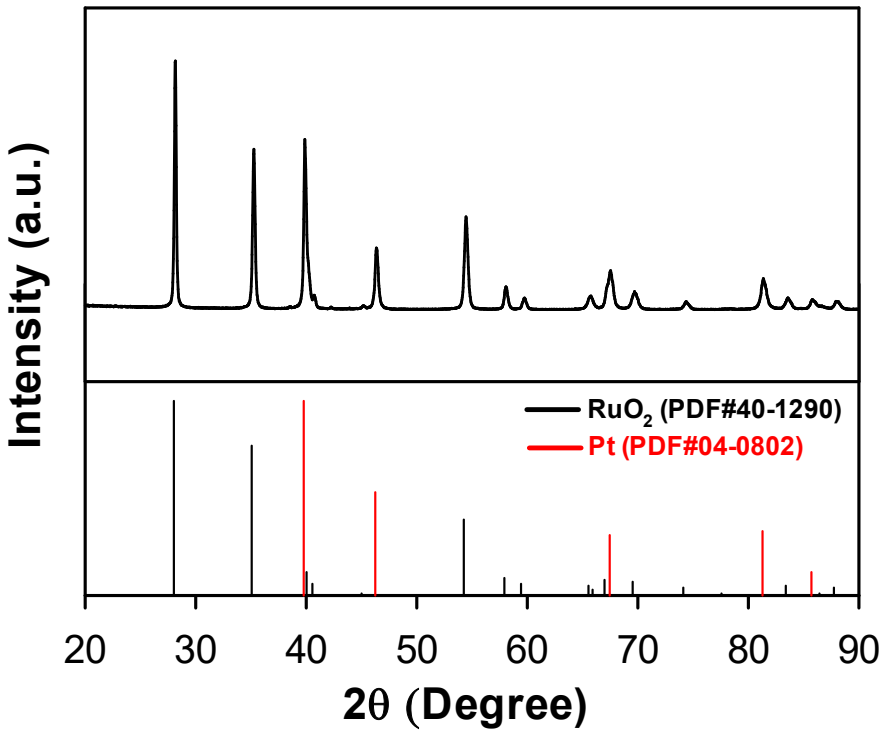

Figure S1. XRD pattern of PR ($Pt_{0.2}Ru_{0.8}O_y$) particles annealed at 800 °C.

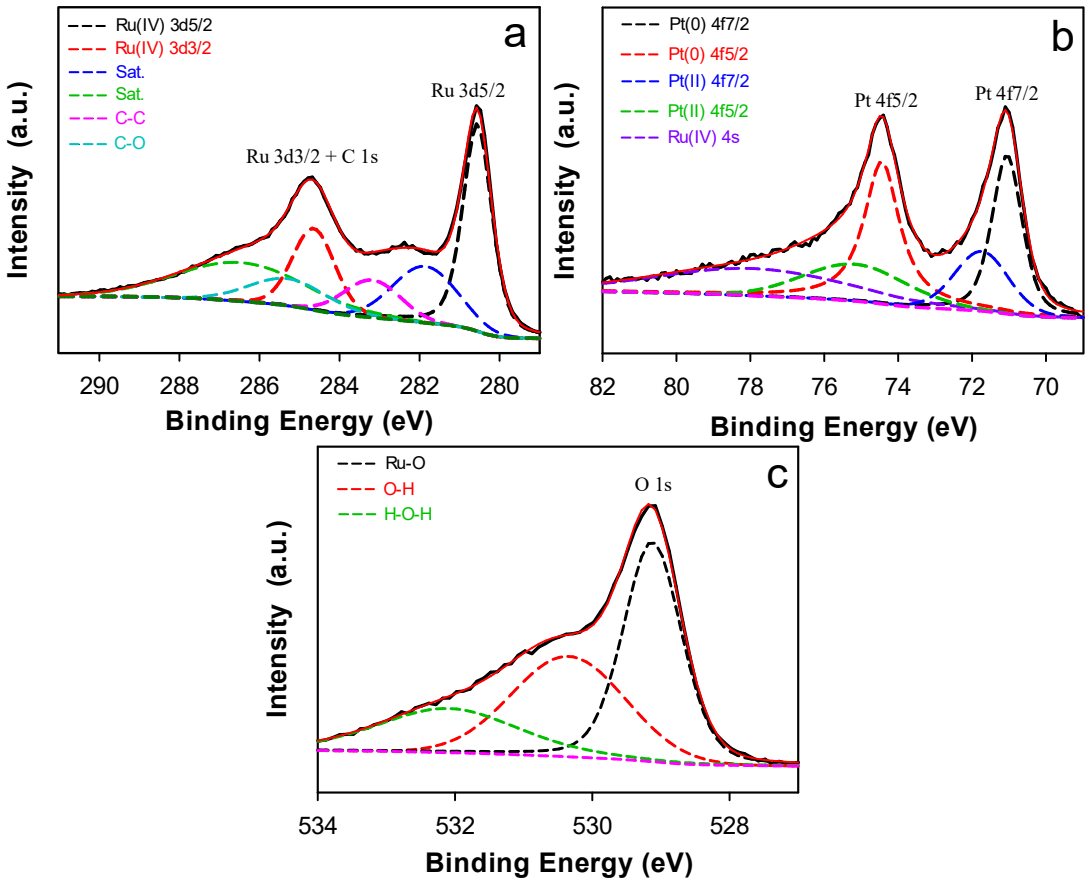

Figure S2. XPS spectra of (a) Ru 3d, (b) Pt 4f, and (c) O 1s) of PR ($Pt_{0.2}Ru_{0.8}O_y$) particles annealed at 800 °C.

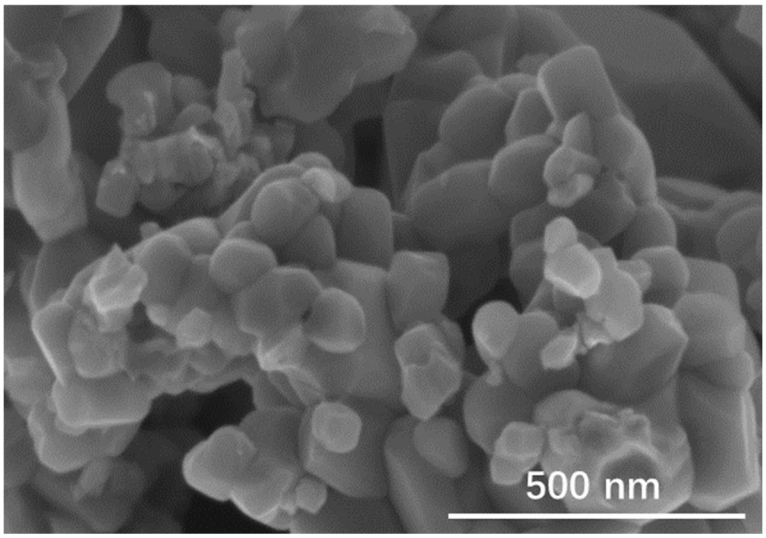

Figure S3. An SEM image of PR ($Pt_{0.2}Ru_{0.8}O_y$) particles annealed at 800 °C.

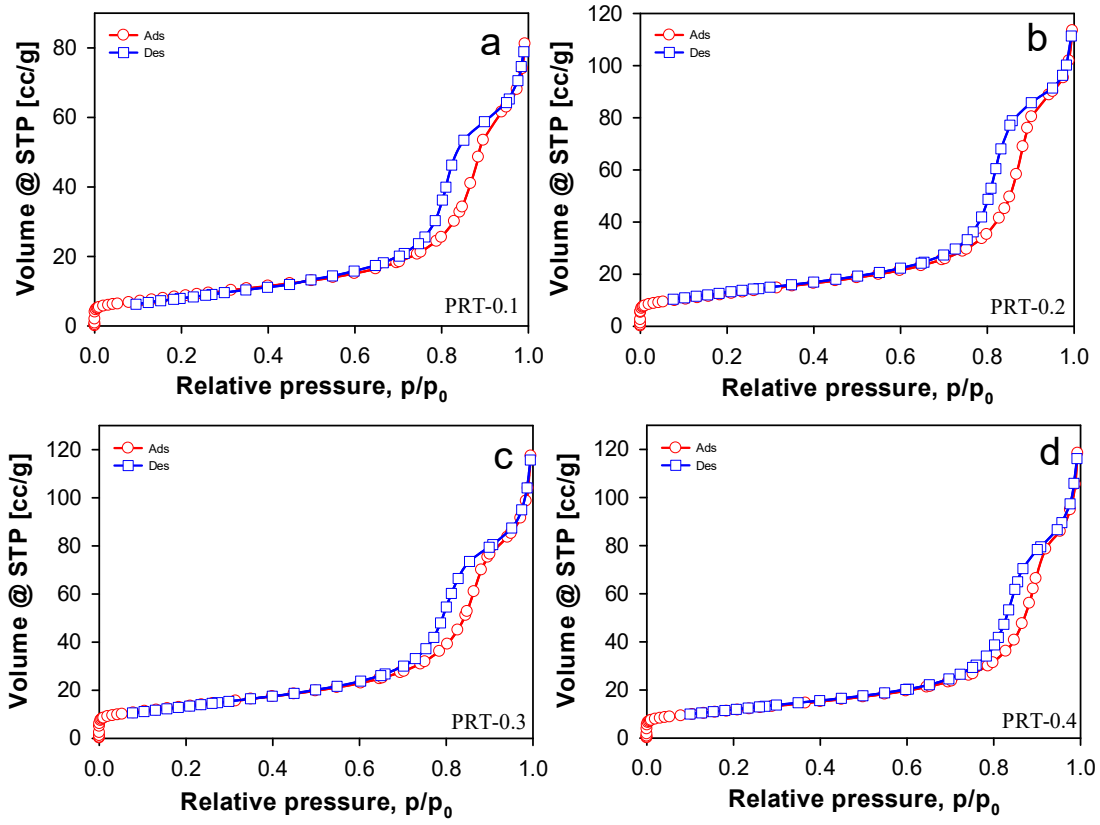

Figure S4. Isotherm N_2 adsorption-desorption curves with (a) PRT-0.1, (b) PRT-0.2, (c) PRT-0.3, and (d) PRT-0.4 samples.

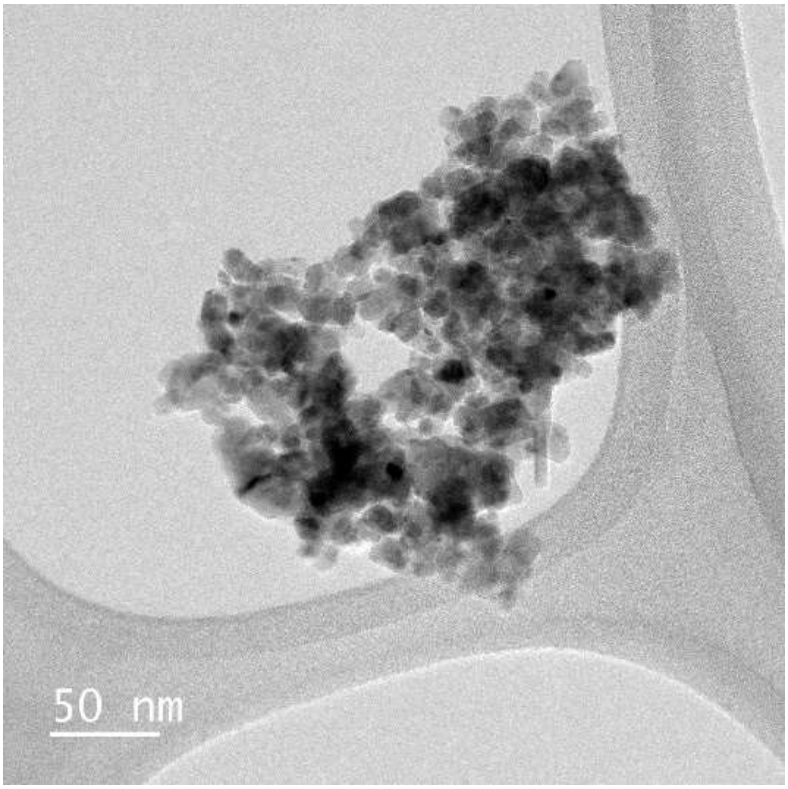

Figure S5. HR-TEM image of PRT ($Pt_{0.06}Ru_{0.24}Ti_{0.7}O_y$) particles annealed at 500 °C.

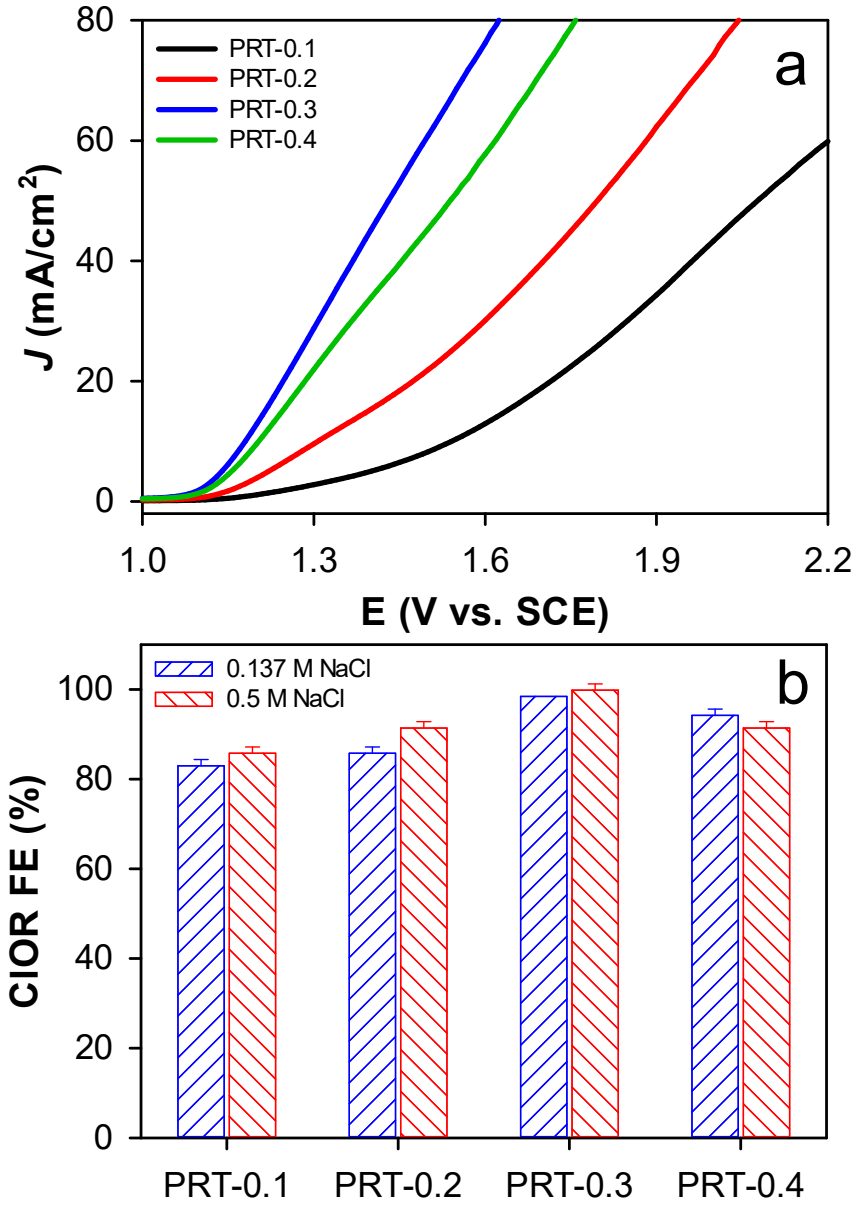

Figure S6. (a) Linear sweep voltammograms of PRT electrodes in 0.5 M NaCl solutions. (b) FE values of ClOR at J = 80 mA cm^{-2} in 0.137 M and 0.5 M NaCl solutions.

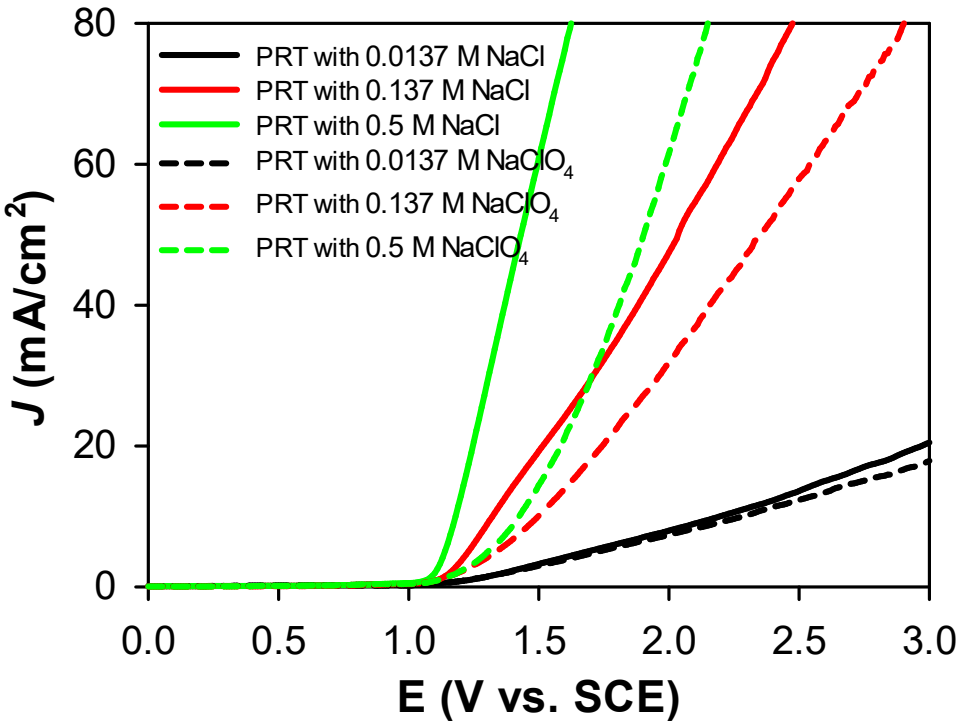

Figure S7. (a) Linear sweep voltammograms with PRT electrodes in NaCl and $NaClO_4$ solutions (0.0137 M – 0.5 M).

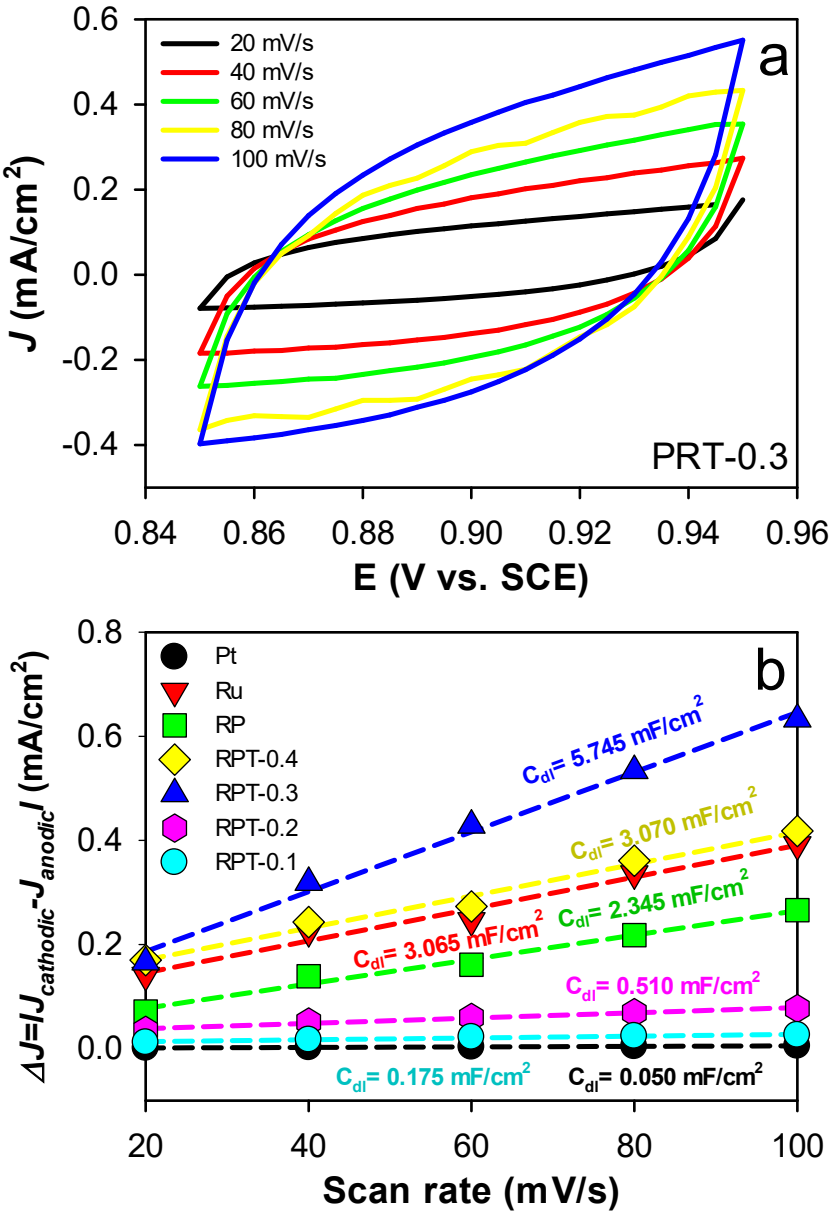

Figure S8. (a) Cyclic voltammograms of RPT-0.3 electrodes and (b) *J* differences between anodic and cathodic *J* values at different scan rates in 0.5 M NaCl solutions.

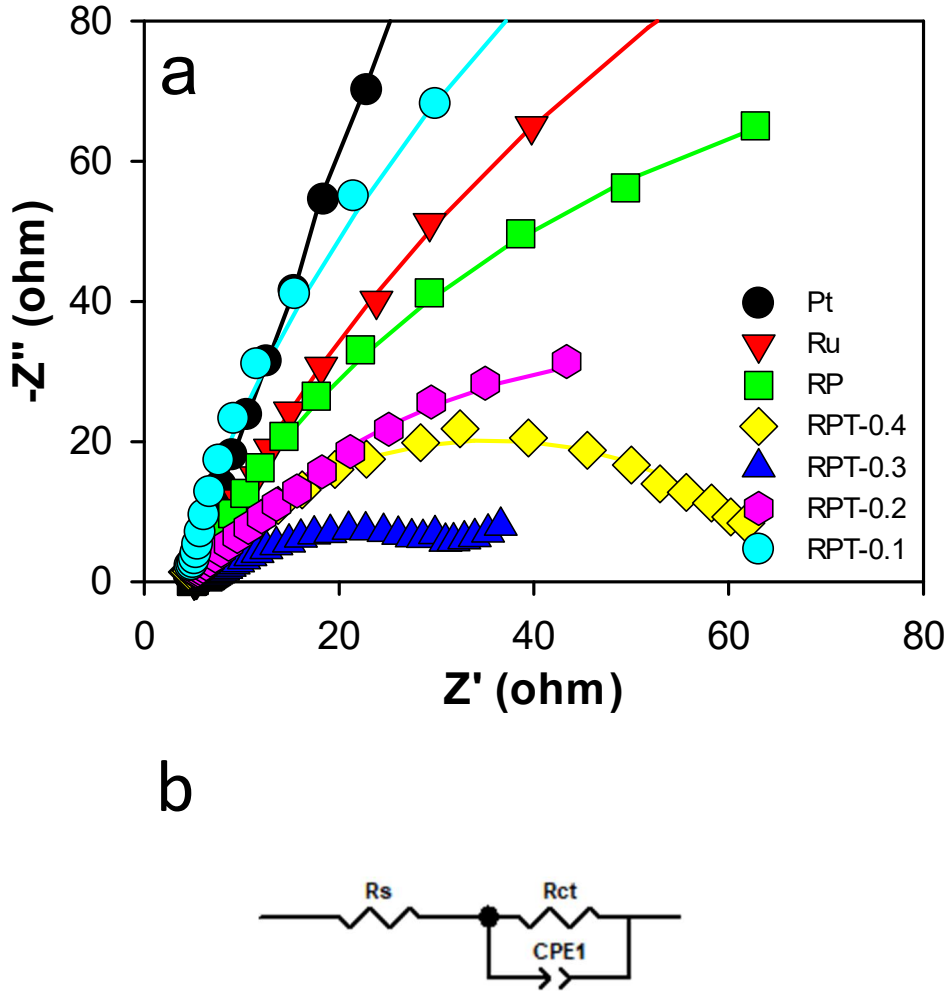

Figure S9. (a) Electrochemical impedance spectroscopy analysis and (b) the equivalent circuit model.

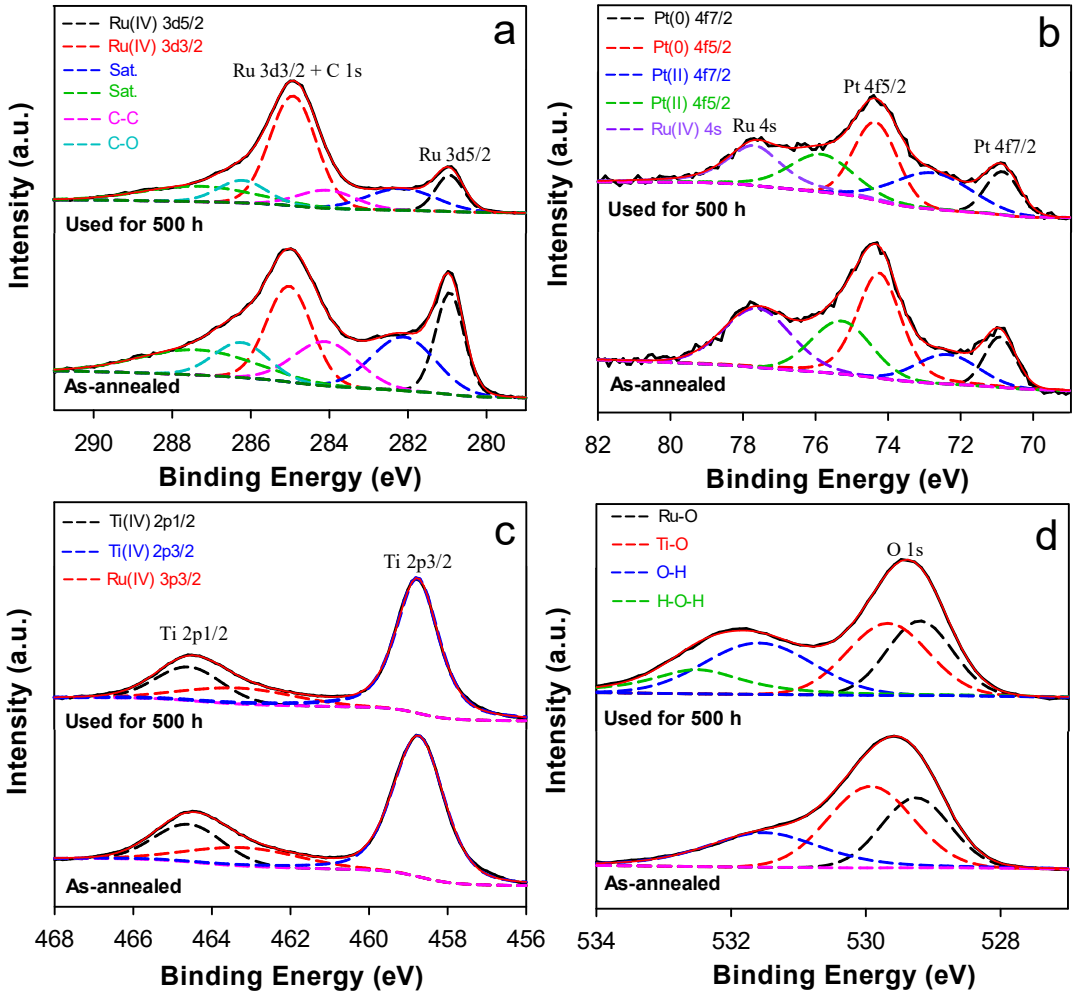

Figure S10. XPS spectra (a: Ru 3d, b: Pt 4f, c: Ti 2p and d: O 1s) of the as-annealed and used PRT electrodes for 500 h at $J = 800$ mA cm^{-2} in 0.941 M NaCl.

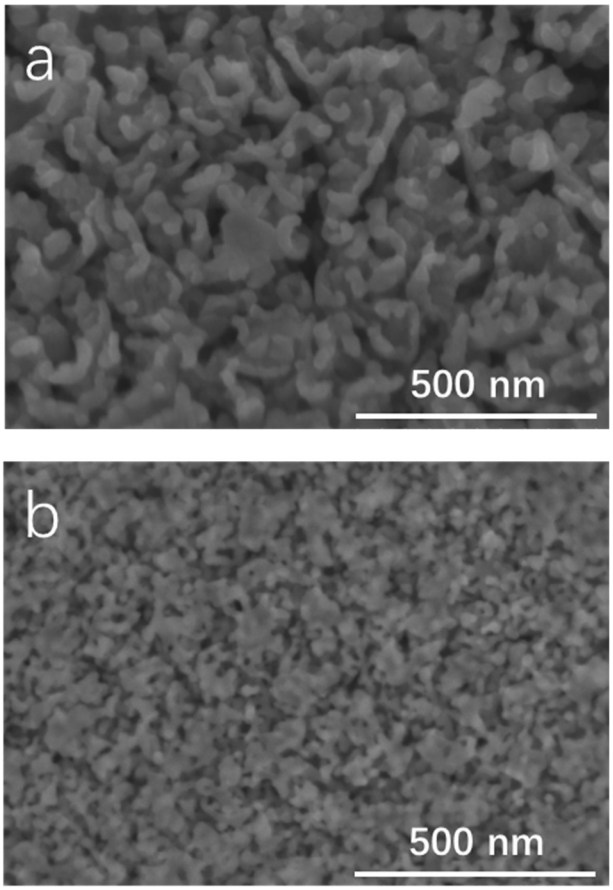

Figure S11. SEM images of (a) MnO_x-200 and (b) MnO_x-400 samples.

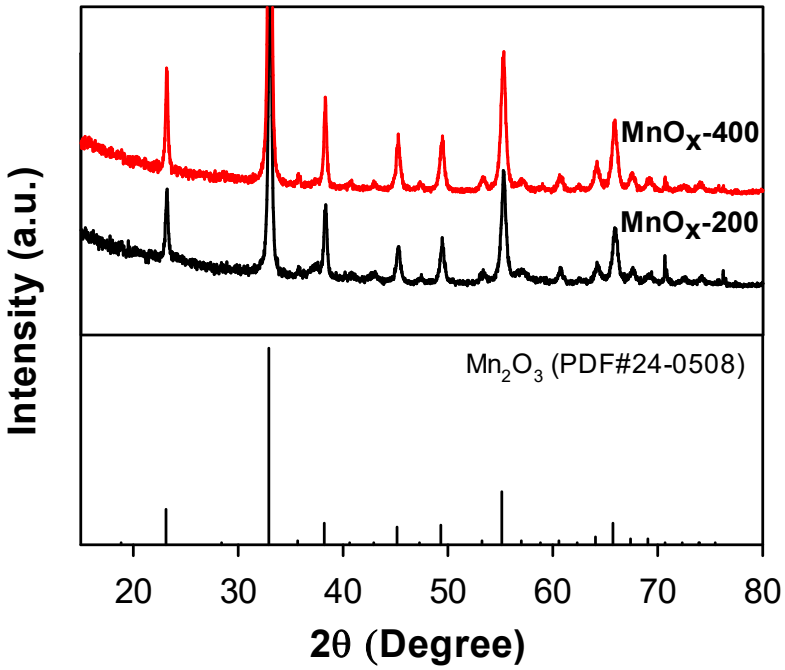

Figure S12. XRD spectra of MnO_x-200 and MnO_x-400 samples.

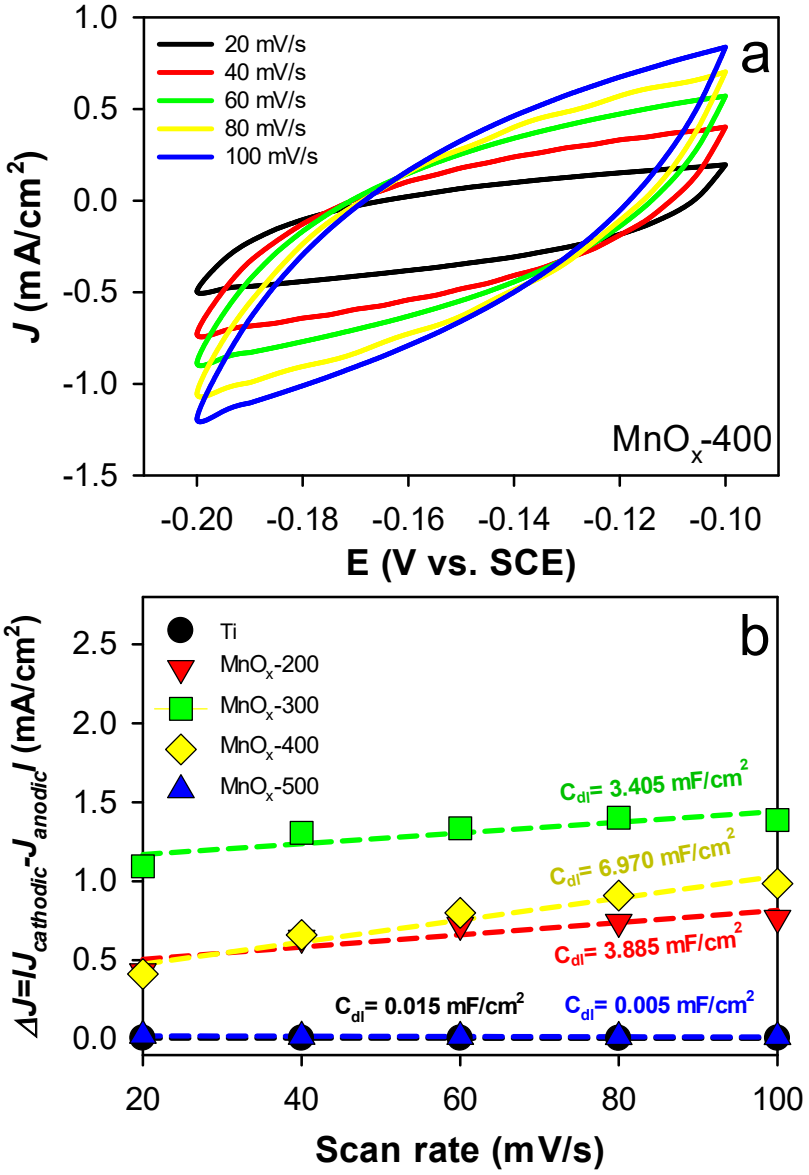

Figure S13. (a) Cyclic voltammograms of MnO_x-400 electrode and (b) differences between anodic and cathodic *J* values at various scan rates in 0.5 M NaCl solutions with 5 mM NaOCl.

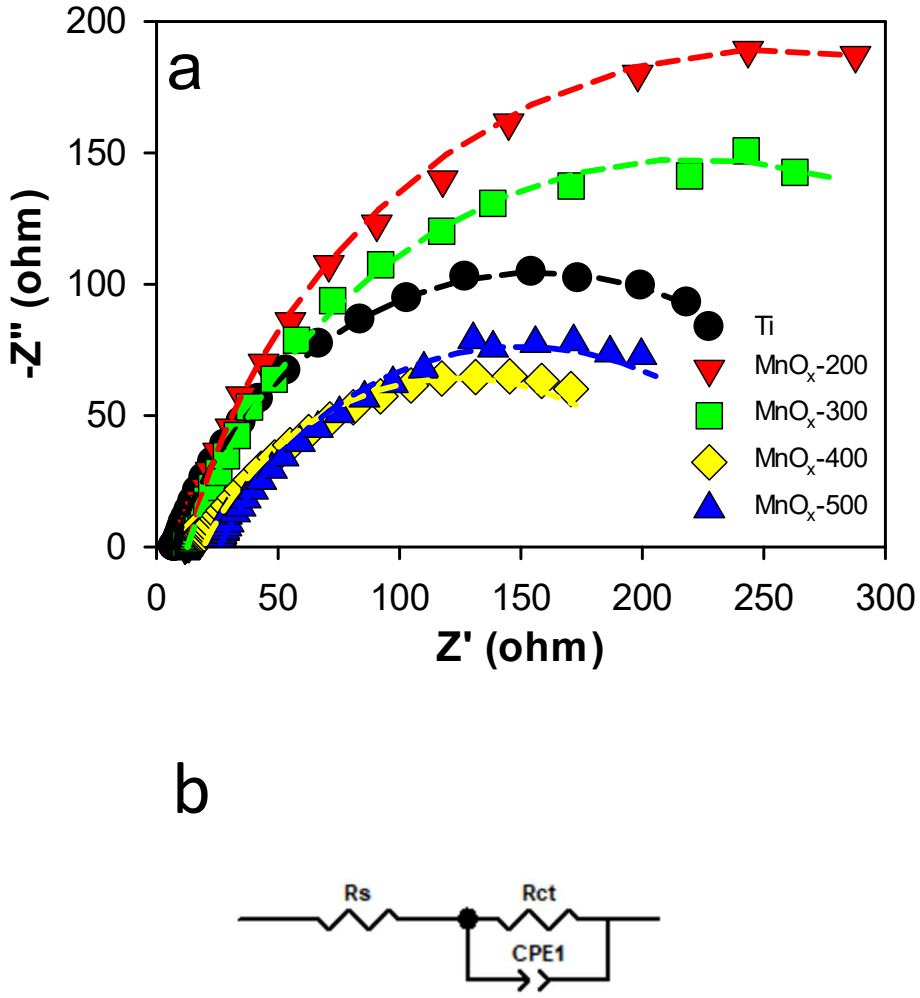

Figure S14. (a) Electrochemical impedance spectroscopy analysis and (b) the equivalent circuit model.

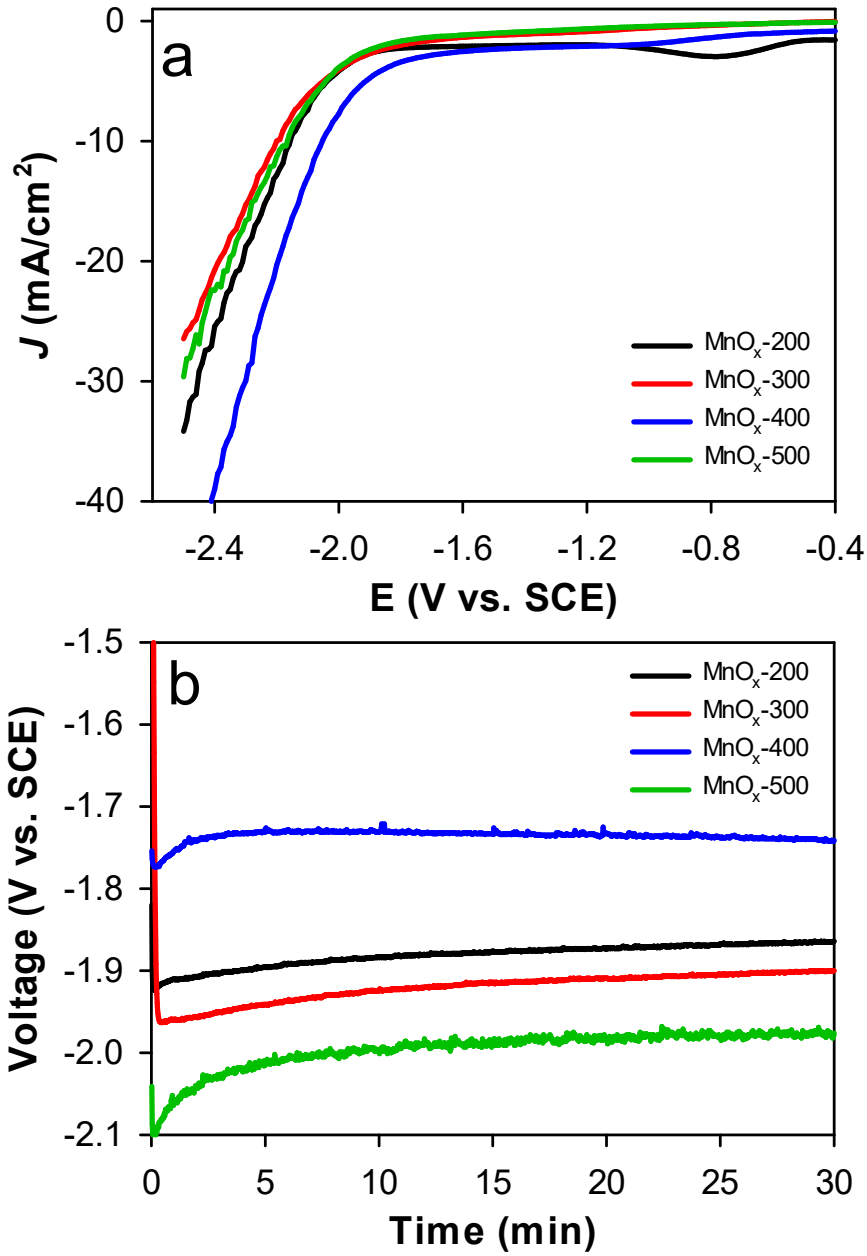

Figure S15. (a) Linear sweep voltammograms and (b) time-profiled changes in *E* values with MnO_x electrodes in 0.5 M NaCl solutions with 5 mM NaOCl.

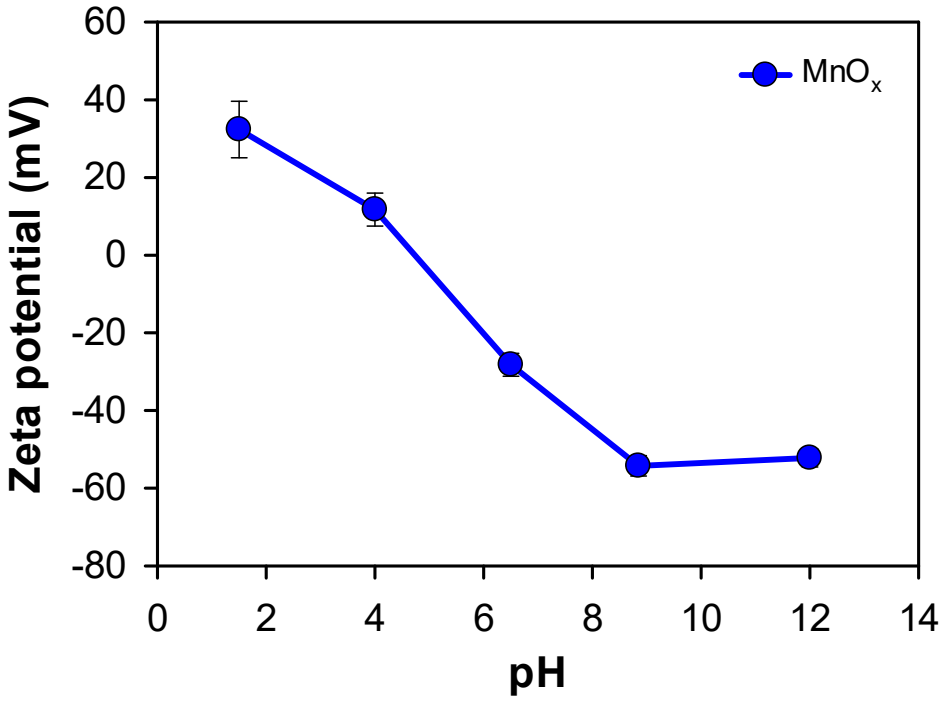

Figure S16. Zeta potentials of MnO_x particles as a function of pH.

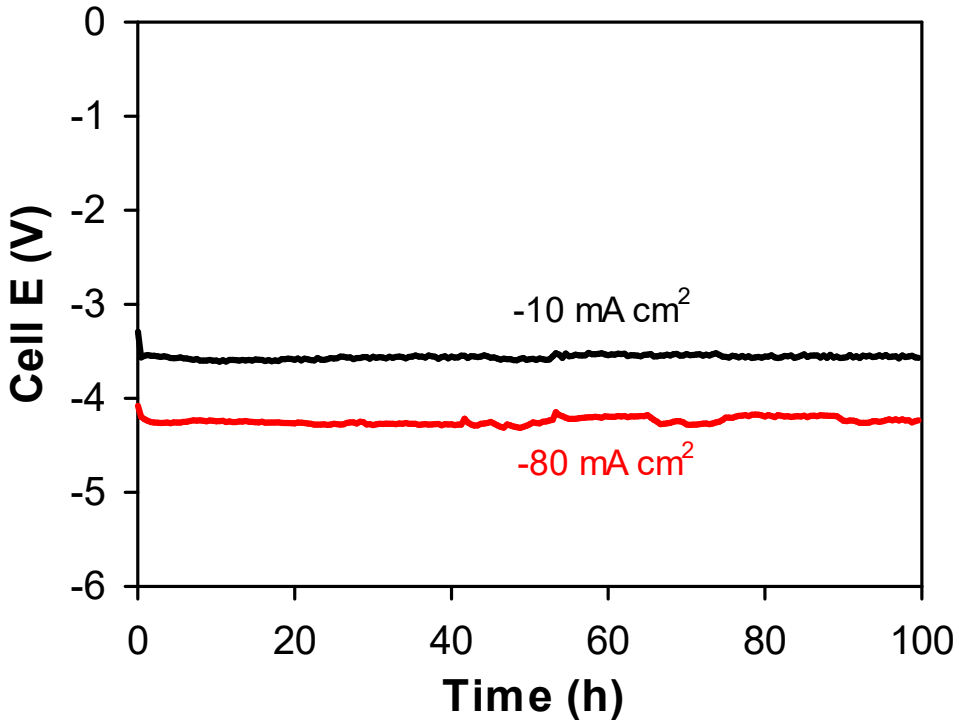

Figure S17. The stability test of MnO_x cathode and Pt anode pair at J_{cell} = 10 and 80 mA cm^{-2} in 0.5 M NaCl solutions.